

The clinical spectrum of Erdheim-Chester disease: an observational cohort study

Juvanee I. Estrada-Veras,¹ Kevin J. O'Brien,² Louisa C. Boyd,¹ Rahul H. Dave,³ Benjamin H. Durham,⁴ Liqiang Xi,⁵ Ashkan A. Malayeri,⁶ Marcus Y. Chen,⁷ Pamela J. Gardner,⁸ Jhonell R. Alvarado Enriquez,¹ Nikeith Shah,¹ Omar Abdel-Wahab,^{9,10} Bernadette R. Gochuico,¹ Mark Raffeld,⁵ Elaine S. Jaffe,⁵ and William A. Gahl^{1,2}

¹Section on Human Biochemical Genetics, Medical Genetics Branch, and ²Office of the Clinical Director, National Human Genome Research Institute, National Institutes of Health, Bethesda, MD; ³Viral Immunology and Intravital Imaging Section, National Institute of Neurological Disorders and Stroke, National Institutes of Health, Bethesda, MD; ⁴Department of Pathology, Mortimer B. Zuckerman Research Center, Memorial Sloan Kettering Cancer Center, New York, NY; ⁵Laboratory of Pathology, Center for Cancer Research, National Cancer Institute, National Institutes of Health, Bethesda, MD; ⁶Laboratory of Diagnostic Radiology Research, Warren Grant Magnuson Clinical Center, National Institutes of Health, Bethesda, MD; ⁷Cardiovascular and Pulmonary Branch, National Heart, Lung, and Blood Institute, National Institutes of Health, Bethesda, MD; ⁸Dental Consult Service, National Institute of Dental and Craniofacial Research, National Institutes of Health, Bethesda, MD; and ⁹Human Oncology and Pathogenesis Program and ¹⁰Leukemia Service, Department of Medicine, Mortimer B. Zuckerman Research Center, Memorial Sloan Kettering Cancer Center, New York, NY

Key Points

- ECD varies in terms of age of onset, clinical presentation, manifestations, organ involvement, disease severity, and survival.
- ECD is a neoplasm and should be adopted by the field of hematology-oncology following the World Health Organization reclassification.

Erdheim-Chester disease (ECD) is a rare, potentially fatal multiorgan myeloid neoplasm occurring mainly in adults. The diagnosis is established by clinical, radiologic, and histologic findings; ECD tumors contain foamy macrophages that are CD68⁺, CD163⁺, CD1a⁻, and frequently S100⁻. The purpose of this report is to describe the clinical and molecular variability of ECD. Between 2011 and 2015, 60 consecutive ECD patients (45 males, 15 females) were prospectively evaluated at the National Institutes of Health Clinical Center. Comprehensive imaging and laboratory studies were performed, and tissues were examined for *BRAF* V600E and MAPK pathway mutations. Mean age at first manifestations of ECD was 46 years; a diagnosis was established, on average, 4.2 years after initial presentation. Bone was the most common tissue affected, with osteosclerosis in 95% of patients. Other manifestations observed in one-third to two-thirds of patients included cardiac mass and periaortic involvement, diabetes insipidus, retro-orbital infiltration, retroperitoneal, lung, central nervous system, skin, and xanthelasma, affecting patients in variable ways. Methods of detection included imaging studies of various modalities. Mutation in *BRAF* V600E was detected in 51% of 57 biopsy specimens. One patient had an *ARAF* D228V mutation, and 1 patient had an activating *ALK* fusion. Treatments included interferon α , imatinib, anakinra, cladribine, vemurafenib, and dabrafenib with trametinib; 11 patients received no therapy. The diagnosis of ECD is elusive because of the rarity and varied presentations of the disorder. Identification of *BRAF* and other MAPK pathway mutations in biopsy specimens improves ECD diagnosis, allows for development of targeted treatments, and demonstrates that ECD is a neoplastic disorder. This study was registered at www.clinicaltrials.gov as #NCT01417520.

Introduction

Erdheim-Chester disease (ECD), first described by William Chester and Jakob Erdheim in 1930,¹ is a rare, group "L" (Langerhans) histiocytosis² characterized by the accumulation of foamy macrophages, chronic inflammation, fibrosis, and organ failure.³⁻⁵ In 2016, ECD was reclassified by the World Health Organization as a hematopoietic neoplasm of histiocytic origin.⁶ Patients often present with bone pain and fatigue, but ECD can manifest with multisystem involvement with cerebellar signs, diabetes

Table 1. Clinical presentation and treatment of 60 NIH patients with Erdheim-Chester disease

Case-sex	Age (y) at:			Presenting finding	Treatment
	NIH visit	First findings	Diagnosis		
1-F	20	16	18	Knee pain, memory loss	PEG-IFN
2-F	30	25	28	Scalp nodules, bone pain	Cladribine
3-F	33	26	28	Ataxia, blindness	Cladribine
4-F	33	22	32	Dizziness, weakness	PEG-IFN
5-M	34	33	33	Hypopituitarism	–
6-M	38	36	37	Testicular pain	Anakinra
7-M	38	18	37	DI	PEG-IFN
8-M	39	37	39	DI, hypogonadism	IFN
9-M	42	24	36	DI, bone pain	IFN
10-M	42	32	42	DI, hypogonadism	PEG-IFN
11-M	44	32	34	DI	IFN
12-M	45	42	44	Bone pain	Vemurafenib
13-M	45	41	41	Bone pain, Horner syndrome	Dasatinib
14-M	45	35	43	Pain, fatigue, depression	Tocilizumab
15-F	46	26	44	DI, seizures	Cladribine
16-M	46	43	43	Pain, fatigue, weakness	Imatinib
17-M	47	26	36	Proptosis	Steroids
18-M	47	40	47	Papilledema	Dabrafenib, trametinib
19-M	47	43	44	Liver and respiratory failure	IFN
20-F	48	46	47	Seizure	IFN
21-F	49	46	48	Weakness	PEG-IFN
22-M	49	34	44	DI, ataxia	PEG-IFN
23-M	50	40	46	DI, fatigue	–
24-F	50	50	50	Skin nodules, lymph nodes	6-MP + Vincristine
25-M	50	46	49	Bone pain	PEG-IFN
26-M	50	47	49	Abdominal mass	–
27-M	51	47	48	DI, hypogonadism	–
28-M	51	45	48	Lung surgery, leg pain	IFN
29-M	51	50	51	Bone pain, fatigue	IFN
30-M	52	51	51	Malaise	Vemurafenib
31-M	53	47	52	DI	Anakinra
32-M	54	51	52	Testicular and bone pain	IFN
33-M	56	40	51	Fatigue, pain	Vemurafenib
34-M	56	50	54	Bone lesion, pain	–
35-M	57	46	50	Pain, fatigue	IFN
36-F	57	53	53	Cardiac tamponade, skin rash	Cladribine
37-F	57	44	44	Periorbital swelling	Methotrexate
38-M	58	55	57	Pain, fatigue	–
39-M	58	48	57	DI, hypogonadism	Cyclophosphamide
40-F	58	47	58	Skin lesions and rash	–
41-M	59	46	49	DI	Imatinib
42-M	59	57	58	Sinusitis	Vemurafenib
43-M	59	48	57	DI	PEG-IFN
44-F	60	55	59	Renal artery stenosis, HT	Anakinra
45-M	61	59	60	Skin nodules	LCH chemotherapy
46-M	61	59	61	Bone pain	IFN

Of the 60 patients included, 51 were white, 4 were Hispanic, 3 were Middle Eastern, 1 was African American, and 1 was Asian.
DI, diabetes insipidus; F, female; IFN, interferon; M, male; PEG-IFN, pegylated interferon.

Table 1. (continued)

Case-sex	Age (y) at:			Presenting finding	Treatment
	NIH visit	First findings	Diagnosis		
47-F	64	62	64	Pericardial effusion	Cladribine
48-F	64	60	63	Sinusitis	Anakinra
49-M	64	60	60	Malaise	–
50-F	64	61	61	Abdominal mass	Vemurafenib
51-M	65	53	54	Ataxia, proptosis	Anakinra
52-M	65	33	57	DI	PEG-IFN
53-M	65	64	64	Malaise	–
54-M	66	64	64	Cerebellar syndrome	–
55-M	67	61	61	None	Anakinra
56-M	68	64	65	Blindness and right-sided weakness	Cyclophosphamide
57-M	69	68	68	Pain, fatigue, ataxia	Methotrexate
58-M	69	67	68	Fatigue, kidney lesion	Methotrexate
59-M	73	51	69	DI	Anakinra
60-M	74	73	74	Incidental imaging findings	–

Of the 60 patients included, 51 were white, 4 were Hispanic, 3 were Middle Eastern, 1 was African American, and 1 was Asian. DI, diabetes insipidus; F, female; IFN, interferon; M, male; PEG-IFN, pegylated interferon.

insipidus, panhypopituitarism, lung and cardiac disease, renal failure, and retroperitoneal fibrosis.⁴⁻⁸ The diagnosis of ECD relies upon clinical, laboratory, histologic, and radiologic studies. Biopsy findings include foamy-to-epithelioid macrophages, often in a fibrotic stromal background, with occasional plasma cells and lymphocytes.^{7,9} Macrophages test positive for CD68, CD163, and factor XIIIa and negative for CD1a and CD207, with 20% positivity for S-100.^{7,9} After diagnosis, some patients with severe forms of disease can succumb to the illness even with treatment. The mortality rate for ECD has been estimated at 60% at 3 years from the time of diagnosis.³

ECD has no standard therapy, although consensus guidelines for clinical management were recently published.⁷ Empiric treatments include anti-inflammatory, immunosuppressive,¹⁰⁻¹⁵ and chemotherapeutic¹⁶⁻²⁰ agents, and recent reports of *BRAF* V600E²¹ and MAPK pathway gene mutations in ECD^{22,23} cells have led to treatment with BRAF and MEK inhibitors.²⁴⁻²⁶

Current knowledge of ECD derives from case reports and retrospective patient series and reviews.¹⁻⁹ We comprehensively and prospectively investigated 60 adults with ECD at the National Institutes of Health (NIH) Clinical Center, and we now present their clinical, radiologic, pathologic, and laboratory characteristics, as well as molecular analyses of biopsy specimens.

Methods

Patients

Patients were enrolled in National Human Genome Research Institute clinical protocol 11-HG-0207, "Clinical and Basic Investigations into Erdheim-Chester disease," and gave written informed consent. All 60 ECD patients admitted for the first time to the NIH Clinical Center between October 2011 and December 2015 were included. Diagnosis was based on a medical history, biopsy samples reviewed by a certified pathologist revealing features of ECD, and imaging studies showing evidence of disease such as osteosclerosis and perinephric stranding. Patients had confirmation of diagnosis prior to admission at the NIH.

Imaging

Radiographs of long bones, radiographs and computed tomography (CT) of the chest, contrast-enhanced cardiac CT, and whole-body technetium-99 bone scans were obtained for all patients. Panoramic dental films were obtained for 51 patients. Contrast-enhanced magnetic resonance imaging (MRI) of the brain, orbits, pituitary, abdomen, and pelvis were obtained in 55 cases; patients with MRI contraindications had CT scans performed instead, and those with intravenous contrast contraindications had imaging studies without contrast. Fluorodeoxyglucose (FDG) whole-body positron emission tomography (PET-CT) scans were obtained in 58 cases; patients with uncontrolled diabetes mellitus were excluded.

Molecular studies

A total of 59 samples were available for molecular testing. The *BRAF* V600E mutation was investigated using polymerase chain reaction–based sequencing of exons 11, 12, and 15 ($n = 25$), allele-specific polymerase chain reaction ($n = 14$), pyrosequencing on a QIAGEN PyroMark Q24 system ($n = 19$), or whole exome sequencing ($n = 1$). See supplemental Materials for more information.

For *BRAF* V600E–negative cases, kinase mutations in *MAP2K1*, *PIK3CA*, *KRAS*, *NRAS*, and *ARAF* were further evaluated using dideoxy sequencing. Urine cell-free DNA and RNA sequencing was performed in selected cases. Whole blood DNA of patients with tissue *BRAF* V600E mutations was examined for the *BRAF* V600E mutation by dideoxy sequencing using an ABI sequencer. For patients with an MAPK mutation on affected tissue, whole-blood DNA was examined for the MAPK mutation.

Statistical analysis

Clinical, imaging, and molecular data were analyzed using descriptive statistics. Continuous variables were summarized as means and intervals, and categorical variables were summarized as frequencies and proportions. Overall survival and manifestations were estimated using Kaplan-Meier plots calculated from date of diagnosis until date of NIH visit. The data collected in this study were available for review by the involved investigators.

Results

Clinical findings

The 60 patients (45 males and 15 females) ranged in age from 20 to 74 years (mean, 53 years) at the time of the evaluation (Table 1).

Age at presentation ranged from 16 to 74 years (mean, 46 years), and mean time to diagnosis was 4.2 years. Three cases had co-occurrence of Langerhans cell histiocytosis (LCH) and ECD. The most common misdiagnosis was sarcoidosis in 8% of patients (5 out of 60). Malignancies were considered in all cases, with lymphoma as the working diagnosis in 60% of patients (36 out of 60), bone cancer in 22% (13 out of 60), brain cancer in 10% (6 out of 60), and orbital lymphoma in 8%. Other differential diagnoses included infectious diseases in 62% of patients (37 out of 60), autoimmune diseases in 27% (16 out of 60), large vessel vasculitis in 22% (13 out of 60), sarcoidosis in 18% (11 out of 60), immunoglobulin G-4 (IgG-4)-related disease in 17% (10 out of 60), and multiple sclerosis in 15% (9 out of 60).

The mean time that the patients had been living with ECD after diagnosis was 2.9 ± 0.4 years (range, 6 months to 11 years), and 38% of patients (23 out of 60) had lived with the disease for 3 years or more prior to their evaluation at the NIH (supplemental Figure 1G). Patients usually exhibited several presenting signs and symptoms; the most common initial findings were diabetes insipidus ($n = 15$; 25%) and bone pain ($n = 10$; 17%). A total of 49 patients (82%) had received drug therapy for ECD; 11 (18%) had mild disease and had not received therapy. Of the 49 treated patients, 40 were on therapy, 6 discontinued therapy secondary to intolerance, and 3 completed the prescribed treatment course. In addition, 73% of the 49 treated patients modified their therapy at least once because of side effects or disease progression (supplemental Table 1).

Upon NIH evaluation, nearly all patients exhibited bone lesions, and approximately half had histiocytic tumors affecting the heart, kidney, lung, or pituitary (Table 2). For patients with a specific tissue affected, Kaplan-Meier plots (supplemental Figure 1) revealed that 50% of patients had involvement of bone at age 55 years, the perinephric region at age 59, diabetes insipidus at age 60, lung at age 61, the retro-orbital area at age 61, and cardiac pseudotumor at age 64. A total of 54 of 60 patients had involvement of multiple organ systems, and 6 patients had ECD affecting only 1 organ system. Comorbidities included coronary artery disease in 39 cases, hypertension in 28, dyslipidemia in 21, diabetes mellitus in 12, Peyronie disease in 2, a second malignancy in 5, and 1 case each of myasthenia gravis, hereditary hemochromatosis, and hydrocephalus.

Bone disease

Bone lesions in ECD are described as osteosclerosis or polyostotic sclerosis as evident on scintigraphic studies of long bones.^{7,8} Bone involvement was present in 95% of cases and involved the appendicular skeleton and occasionally the axial skeleton. Technetium-99 bone scans (Figure 1A) and FDG PET-CT scans (Figure 1B) revealed increased uptake in affected areas. Long bone osteosclerosis was detected on plain radiographs (Figure 1C-D), CT (Figure 1E), and MRI (Figure 1F). Panoramic imaging showed bilateral midroot radiolucencies in the maxilla and mandible (Figure 1G) in 47% of cases ($n = 51$). For long bones, bilateral involvement was seen in the femur in 88% of patients, tibia in 88%, humeri in 42%, and radii in 42%. In addition, the skull, vertebrae, mandible, pelvis, and ribs occasionally contained lesions, and MRIs of the head showed thickening of the facial bones and maxillary sinuses in 50% of cases. Technetium-99 bone scan was the imaging modality with the highest sensitivity in detecting bone

Table 2. ECD organ involvement in NIH patients and in the literature

Organ system and clinical findings	NIH patients,* n (%)	Veyssier-Belot et al† (%)	Haroche et al‡ (%)
Bone	57 (95)	NR	96
Kidney	39 (65)	27	68
Periaortic encasement	37 (62)	NR	66
Hypogonadism	36 (60)	NR	NR
Lung	31 (52)	14	43
Bone pain	28 (47)	47	40
Maxilla and mandible§	24 (47)	NR	NR
Diabetes insipidus	28 (47)	29	25
CNS disease infiltration	23 (38)	17	51
Retro-orbital area ± exophthalmos	15 (27)	29	25
Heart (pseudotumor in RA)	22 (37)	NR	19
Xanthelasma	20 (33)	19	28
Skin	15 (25)	10	NR
Pericardial disease	5 (8)	7	42

CNS, central nervous system; NR, not reported; RA, right atrioventricular groove.

*Number of patients out of the 60 patients prospectively investigated.

†Data included 59 cases (1996).³

‡Data included 122 historical cases (2014).⁴

§Panoramic dental imaging was performed in 51 cases.

disease when compared with plain film radiographs. Plain radiographs detected osteosclerosis in the radii in 42% of patients (26 out of 60) and in the femur and tibia in 60% (36 out of 60) and 65% (39 out of 60), respectively. In comparison, T-99 bone scans showed increased radiotracer uptake in the radii in 47% of the cases (28 out of 60) and in the femur and tibia in 88% (53 out of 60). There was no evidence of bone disease in 5% of the cases. In our series, 82% of patients had received therapy prior to our evaluations. Approximately half of the affected individuals described deep, dull bone pain, especially in the knees.

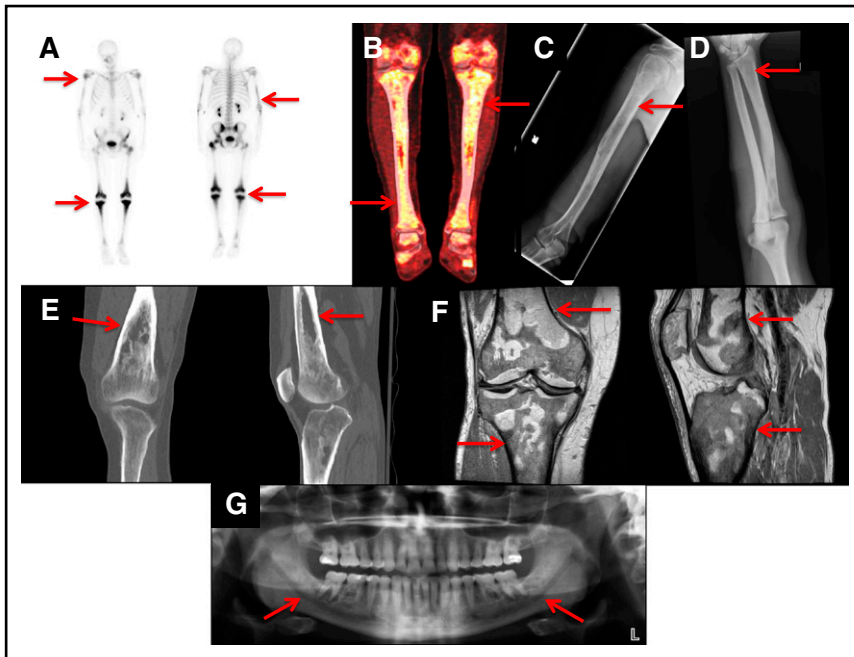
Cardiovascular disease

Coated aorta or circumferential encasement of the aorta (Figure 2A-C) was apparent in 62% of patients. The most common cardiac manifestation was pseudotumor of the right atrioventricular groove, apparent on cardiac CT (Figure 2D-E) in 37% of patients. Rarely involved vessels included the portocaval system, causing portal hypertension in 1 case and mesenteric vessel disease producing bowel ischemia in 3 cases. Stents were used to bypass the stenosis. A total of 5 patients had pericardial involvement; 2 had cardiac tamponade, and 4 needed pacemakers for abnormal rhythms. None of the cases had evidence of valvular disease or cardiac failure.

Retroperitoneal involvement

One-third of patients had a history of renal impairment prior to their NIH visit. A total of 65% of patients (39 out of 60) exhibited encasement of the kidneys and involvement of the retroperitoneal space (Figure 2F-G), causing renal artery stenosis in 54% of cases (21 out of 39) and ureteropelvic junction obstruction in 51% of that group of patients (20 out of 39); 13 cases were affected by both renal artery stenosis and ureteropelvic junction obstruction. Hypertension controlled by renal artery stents was reported in 4 cases and hydronephrosis needing ureteral stents in 6. Three

Figure 1. Bone lesions in ECD. The red arrows show: (A) Whole-body bone scan with technetium-99 showing avid uptake in the knees and left hip of an ECD patient. Less intense uptake occurs bilaterally in the humeri and distal tibiae. (B) FDG PET-CT scan showing increased FDG uptake in the knees and proximal and distal tibiae. (C) Bone radiograph showing cortical osteosclerosis in the right humeri. (D) Bone radiograph showing cortical osteosclerosis in the distal right radius. (E) CT scan of the right knee of an ECD patient showing cortical osteosclerosis and mottled appearance of the bone. (F) MRI scan of the right knee of an ECD patient showing serpiginous areas of T1 signal hypointensity, indicative of osteosclerosis. (G) Panoramic radiograph showing bilateral osteosclerosis of the mandible and maxillary sinus disease.



patients had a history of requiring nephrostomy tubes. In these cases, renal function was impaired, but neither renal transplantation nor dialysis was under consideration.

Endocrine abnormalities

Diabetes insipidus was confirmed in 47% of patients, all of whom were treated with vasopressin (10 μ g once or twice daily). Nevertheless, urine volume was 2557 ± 1533 (mean \pm standard deviation) mL/day, with a range of 700 to 7375. Mean urine osmolality was 493 mOsm/kg, mean serum osmolality was 298 mOsm/kg, and mean urine specific gravity was 1.02. Even

though diabetes insipidus was diagnosed in 47% of patients, pituitary MRI with contrast showed pituitary stalk thickening in 14 out of 55 cases (25%).

Other endocrine abnormalities included hypogonadism in 60% of patients. Of the 15 females in the study, 6 had a history of amenorrhea or infertility, and 30 of the 45 males had hypogonadism confirmed by decreased total or free testosterone levels. Follicle stimulating hormone and luteinizing hormone were increased in nearly half of the patients. Insulin-like growth factor levels were abnormal (high or low) in one-third of the cases, 22% of patients

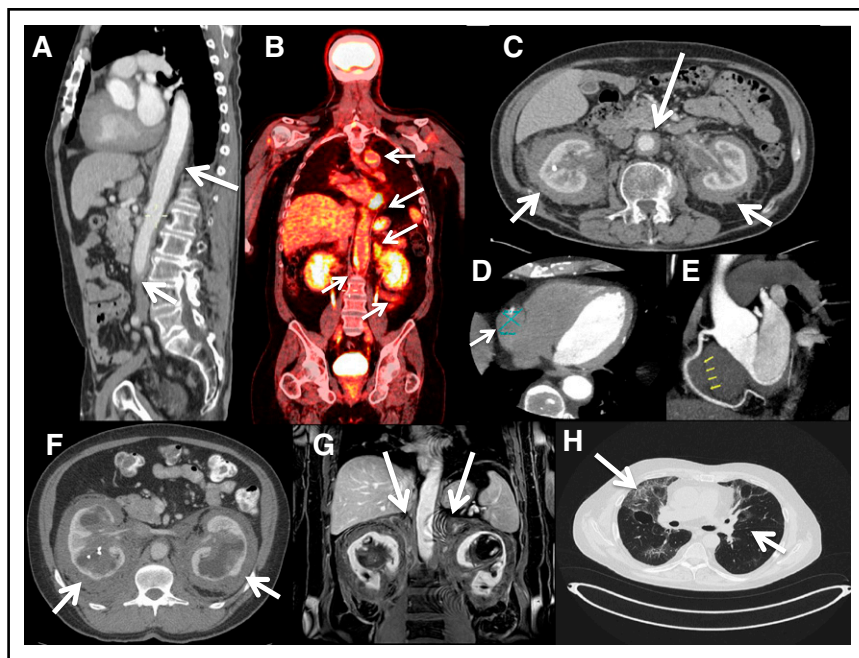


Figure 2. Cardiovascular, retroperitoneal, and lung images of ECD patients. (A) Sagittal reconstruction postcontrast CT demonstrates encasement of the thoracic aorta down to the bifurcation. (B) Coronal FDG PET-CT scan showing increased FDG uptake in the thoracic and abdominal aorta. Symmetrically encased kidneys “hairy kidney” showing increased FDG uptake. (C) Axial CT with contrast demonstrates mass-like enhancement encasing the kidneys symmetrically (“hairy kidney”). In addition, there is circumferential encasement and narrowing of the abdominal aorta (arrow). (D) Cardiac CT showing partial encasement of the right coronary artery. (E) Cardiac CT showing partial encasement of the right coronary artery. (F) Axial postcontrast CT image of the upper abdomen demonstrating mass-like perinephric stranding surrounding the kidneys with bilateral hydronephrosis. Hyperdense material within the right collecting system is a ureteral stent. (G) Postcontrast coronal MRI image of the kidneys demonstrating extension of the perinephric mass into the adrenal bed and encasement of the adrenals (arrows). (H) High-resolution CT of the chest showing interstitial fibrosis.

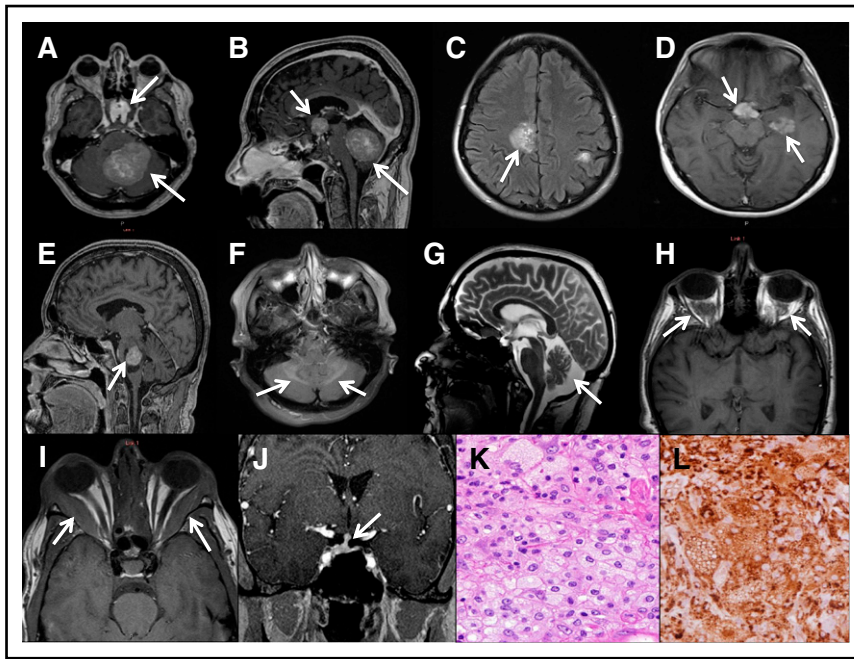


Figure 3. Brain images in ECD. (A) Axial post contrast brain MRI showing suprasellar and cerebellar involvement in a patient with ECD. (B) Sagittal post contrast brain MRI (from panel A) showing suprasellar and cerebellar tumors in a patient with ECD. (C) Axial fluid attenuated inversion recovery brain MRI showing ECD tumors in cerebral hemispheres. (D) Axial fluid attenuated inversion recovery brain MRI showing ECD tumors in cerebral hemisphere. (E) Sagittal post contrast brain MRI showing an ECD tumor with cystic components in the midbrain-pons of a patient with ECD. (F) T2 fluid attenuated inversion recovery MRI image showing increased symmetrical signal intensity in the cerebellum. (G) Neurodegeneration and atrophy of the cerebellum in a patient with ECD seen on brain MRI. (H) Orbital involvement with tissue accumulation in the intraconal space secondary to histiocytes accumulation in ECD. (I) Orbital involvement showing increased thickening of the lateral rectus muscle. (J) Pituitary stalk is thickened secondary to macrophage accumulation in ECD and deviated to the right. (K) Hematoxylin and eosin stain for brain lesion showing foamy macrophages and inflammation in brain mass biopsy specimen (original magnification $\times 40$). (L) CD68 KP-1 stain of panel K highlighting the foamy macrophages (original magnification $\times 40$).

had hypothyroidism, and 7% had adrenal insufficiency. Adrenal gland involvement was present in 21 cases (35%) (Figure 2G). Occasional abnormalities in parathyroid, growth, adrenocorticotropic, and prolactin hormones were seen.

Neurologic and cranial involvement

Neurologic signs or symptoms were present in 92% of patients (15% presented with a neurologic complaint) and 87% (55 patients) had an abnormal head MRI. Clinical involvement included mild cognitive impairment (40%) or dementia (8%), brainstem findings (52%), cerebellar ataxia (40%), sensorineural hearing loss (8%), seizures (8%), headaches (23%), and peripheral neuropathy (56%). The most prominent bulbar symptoms were diplopia (15%), dysarthria (14%), and dysphagia (13%). Neuroradiologic features included atrophy in 30% of patients (Figure 3G), cerebral masses in 20%, cerebellar masses in 16% (Figure 3A-E), retro-orbital masses in 27% (Figure 3H), and dural thickening in 7%. A small number of cases had infiltrative T2-weighted fluid attenuated inversion recovery lesions (Figure 3F) and extraocular muscle thickening (Figure 3I). Periorbital masses were frequently space occupying and caused visual impairment (15 cases), gaze palsies (9 cases), proptosis (3 cases), and papilledema (1 case). Pituitary abnormalities included pituitary stalk thickening in 14 cases (Figure 3J), T2 hypointensities in 7 cases, and suprasellar masses in 5 cases. Brain mass pathology revealed foamy macrophages (Figure 3K-L). Overall, neurologic disease in ECD was more prevalent than previously reported,^{3,4,7,8,27} and we have expanded its spectrum to

involve neurodegeneration, seizures, dural and white matter non-displacing lesions, and extracranial space-occupying lesions.

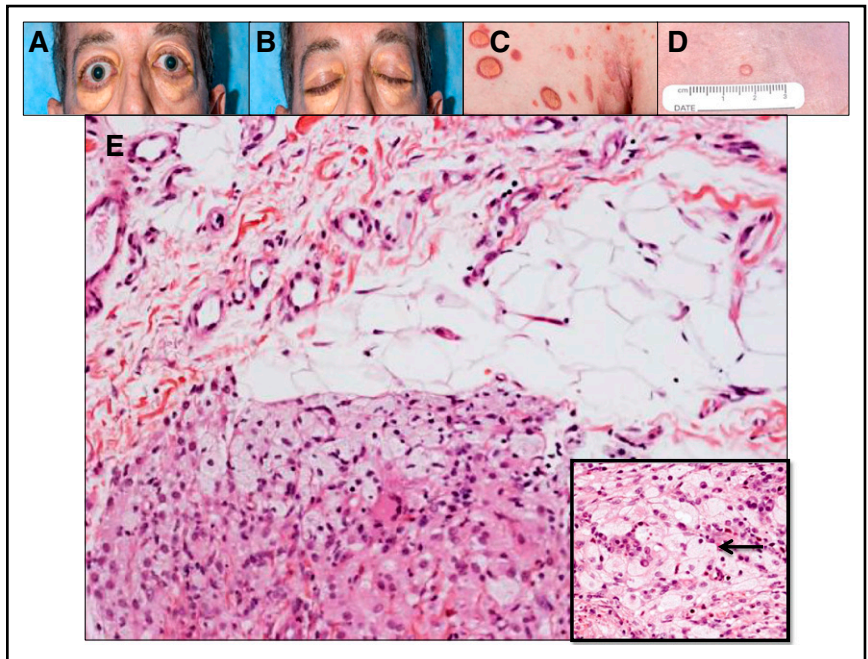
Pulmonary manifestations

Patients were generally asymptomatic from pulmonary disease, but some experienced dyspnea with exertion. Interstitial fibrosis with reticular pattern was apparent on high-resolution chest CT (Figure 2H) in 52% of patients; plain films of the chest did not reveal lung disease. Pulmonary function tests showed a restrictive pattern in 30% and an obstructive pattern in 7% of patients. The mean diffusing capacity of the lungs for carbon monoxide level was 23.0 mL/mm Hg per minute, with a range of 8.5 to 36.

Skin

Periorbital xanthelasmas (Figure 4A-B), presenting in adulthood and increasing in size, occurred in one-third of cases. Other skin lesions (Figure 4C-D), present in 25% of cases, resembled those of juvenile xanthogranuloma (JXG), diffuse xanthoma, reticulohistiocytoma, or a rash resembling LCH. The upper trunk and extremities were commonly affected areas. Lesions were found on the dorsal aspect of the hands in 2 cases and on the dorsal aspect of the feet in 1 case. Pathology revealed foamy macrophages, inflammatory cells, fibrosis (Figure 4E), and Touton giant cells in the biopsied lesions. Pain and pruritus responded partially to therapy with interferon, especially in cases involving periorbital xanthelasmas and JXG-like lesions.

Figure 4. Skin findings in ECD. (A) Periorbital xanthelasmas in a patient with ECD. Note mild exophthalmos secondary to retro-orbital mass. (B) Upper lid xanthelasmas are apparent when the patient's eyes are closed. (C) Skin lesions containing foamy macrophages negative for S-100 protein but with activating ALK gene fusion. (D) Skin lesion positive for BRAF V600E mutation. (E) Foamy macrophages in skin lesion. Inset shows lipid-laden macrophages interspersed with inflammatory cells (original magnification $\times 20$; hematoxylin and eosin stain).



Other organs

One patient had histological evidence of ECD in the liver confirmed by biopsy (not shown), and another patient had pancreatic encasement requiring enzyme replacement therapy.

Other imaging

A total of 58 clinical torso/extremity PET scans with FDG were available for analysis (Figures 1B and 2B). Two patients did not have PET scans because of uncontrolled diabetes mellitus. A total of 54 scans (93%) showed increased FDG uptake in one or more organs. The most common findings were increased standardized uptake values in bilateral femur (74%), bilateral tibia (67%), the bilateral perinephric area (35%), and bilateral humeri, lungs, and mediastinum (24% each). A total of 4 scans showed physiologic uptake; 2 patients had completed therapy with cladribine, and 3 had single-organ ECD. The PET scans were performed at the NIH, and results were influenced by the therapeutic history.

Pathology

The 60 patients underwent a total of 79 tissue biopsy procedures. A total of 76 biopsies exhibited pathological findings consistent with ECD, and 3 biopsies exhibited findings consistent with LCH (supplemental Table 2). Most biopsies involved perinephric or retroperitoneal tissue, bone, or skin, but over 20 different areas of the body were sampled. More than 1 biopsy was needed in 17 cases to establish the diagnosis. Foamy histiocytes (Figures 4E and 3K) were present in all biopsy samples of patients with ECD. Fibrosis was reported in 94% of biopsy specimens, and Touton giant cells were found in 92%. Histiocytic cells were sometimes associated with a minor population of lymphocytes, neutrophils, eosinophils, or plasma cells. Emperipolesis was not observed. The lesions lacked necrosis, mitoses, nuclear atypia, and well-formed granulomas. All specimens were positive for CD68 and 93% of specimens (27 out of 29) were positive for CD163, while only 4%

were positive for CD1a. S100 was positive in 9% of ECD samples and in all LCH samples. Of 18 biopsy specimens tested for factor XIIIa, 17 were positive. Stains for IgG-4-related disease were performed in 7 cases and were negative. The 3 cases that exhibited features of ECD and LCH had, in 1 case, pathology suggestive of ECD in a skin biopsy specimen and LCH in a bone biopsy specimen. A second case had ECD in orbital tissue and LCH in bone. The third case had ECD in perinephric tissue and LCH in colon tissue.

Laboratory findings

Laboratory findings included low hemoglobin values (62%), elevated C-reactive protein (47%), and elevated erythrocyte sedimentation rates (42%) (supplemental Table 3). Ferritin levels were mostly normal. Pro-brain natriuretic peptide was elevated in 50%. Of the 50 cases in which vitamin B12 was measured, 46% had values < 400 pg/mL. A positive anti-nuclear antibody with no clinical evidence of an autoimmune disorder was present in 14 patients. Lupus anticoagulant was positive in 8 of the 9 cases tested after screening coagulation studies. These patients did not have a history of thromboembolism, ischemic events, or fetal losses.

Molecular studies

Of the 60 ECD patients, 57 had interpretable *BRAF* sequencing of affected tissues; 31 (52%) were positive for *BRAF* V600E (14 perinephric tissue, 7 skin, 5 bone, and 1 pericardial, pleural, orbital, cerebellar, and pituitary tissue each). Of the 3 cases with ECD and LCH, 2 cases had interpretable *BRAF* sequencing of the LCH-affected tissue and were positive for *BRAF* V600E. The ECD-affected tissue of these cases was also positive (supplemental Table 4A-B). Three cases did not have tissue available. A total of 23 patients (38%) were *BRAF* wild type on tissue sampling, but the *BRAF* V600E mutation was detected on sequencing of urine cell-free DNA in 2 cases, yielding a total of 55% cases positive for *BRAF* V600E. None of the 57 patients had germline *BRAF* mutations. Of

the 21 wild-type *BRAF* V600 cases, 12 tissues (4 bone, 1 bone marrow, 2 perinephric tissue, 2 skin, and 1 of lung, pericardium, and soft tissue) had sufficient DNA for further evaluation. The *ARAF* D228V mutation and an activating *ALK* fusion (*KIF5B-ALK*) were found in 1 case each.

Treatments

The most common active therapies were interferon α 2b ($n = 16$) and anakinra ($n = 7$) (supplemental Table 1). Four patients were treated with vemurafenib. Imatinib, methotrexate, and cladribine were used in 2 patients each. Cyclophosphamide, tocilizumab, dasatinib, 6-mercaptopurine with vincristine, vinblastine, steroids, and dabrafenib with trametinib were used in 1 patient each. The most common therapy discontinued secondary to side effects was interferon α 2b; anakinra had the fewest reported side effects. Prior to confirmation of ECD, 33% of patients (20 out of 60) received high-dose steroids, most commonly IV methylprednisolone followed by oral steroid taper.

Response to therapy was difficult to determine, because multiple therapies were used over the years. However, after patient examination and comparison of our imaging with previous body imaging in the cases that had received therapy ($n = 49$), 29 cases had evidence of stable disease. Partial response and progression of disease were evident in 10 cases each. Stable disease was seen in 78% of cases (14 out of 18) treated with interferon α , in 57% (4 out of 7) of cases treated with anakinra, in 2 cases treated with vemurafenib, and in 2 cases treated with methotrexate. Partial response was seen in 1 case ($n = 18$) treated with interferon α and in 1 case treated with imatinib. No partial response was reported with anakinra. Six patients with partial response were treated with cladribine, and 3 were treated with vemurafenib. Progression of disease was seen in 17% of patients (3 out of 18) treated with interferon α 2b and 43% of patients (3 out of 7) treated with anakinra. Other patients with progression of disease received cyclophosphamide ($n = 2$), 6-mercaptopurine with vincristine ($n = 1$), and dasatinib ($n = 1$). Palliative radiation was given in 6 cases with no response. A total of 11 patients did not receive therapy because of mild disease that did not interfere significantly with the patient's quality of life.

Discussion

Histiocytes are tissue-resident cells derived from circulating CD34⁺ myeloid bone marrow precursor cells of the mononuclear phagocytic systems; they include macrophage and dendritic cells. In histiocytoses, these cells accumulate because they fail to apoptose.^{2,5,9} Histiocytoses, which differ in clinical presentation, progression, response to therapy, and outcome, have been historically classified as Langerhans cell or non-Langerhans cell subtypes, with dendritic, macrophage and monocytic, and malignant forms.^{9,13} Within this classification, ECD falls into the non-Langerhans group of histiocytoses. A new classification for histiocytic disorders was proposed by Emile et al² in which LCH and non-LCH histiocytoses comprise the group L (Langerhans) histiocytoses because of the clinical and molecular similarities between these entities. In our cohort, 3 cases had co-occurrence of ECD and LCH. The US-based Erdheim-Chester Disease Global Alliance has identified 170 affected individuals in the United States and 142 abroad.

The rarity of ECD impedes timely diagnosis, which requires a high index of suspicion; no specific immunohistochemical markers exist. The cells have the immunophenotype of reactive histiocytes.

Because the cells lack cytological atypia, the neoplastic nature of the proliferation is often not recognized, and it is the characteristic clinical features that often prompt consideration of the diagnosis. Fine cytoplasmic lipid vacuoles filling the cytoplasm are the most typical cytological feature (foamy macrophages), although their absence does not rule out ECD.^{2-9,13} The cells lack markers of Langerhans cells. In general, foamy-to-epithelioid macrophages that stain positively for CD68, CD163, CD14, and factor XIIIa are highly suggestive of ECD, more so when proper clinical and imaging evaluations are correlated. Other findings include Touton or multinucleated giant cells, anti-factor XIIIa positivity, and absence of Birbeck granules.⁷ Lack of appreciation of the histological and clinical features delays diagnosis; in our cohort, the mean time between first signs and diagnosis was 4.2 years. Communication among clinicians, radiologists, and pathologists is vital.

Many ECD patients are misdiagnosed with Paget disease of the bone, lymphoma, multiple sclerosis, sarcoidosis, pituitary adenoma, IgG-4 sclerosing disease, or other granulomatous disorders. Histiocytic sarcomas and lysosomal storage diseases such as Gaucher disease and Fabry disease and various histiocytoses may also be suspected.^{7,27-31} LCH, with its pathognomonic cell features, can be differentiated from ECD by staining for CD1a and langerin.^{7,13} Rosai-Dorfman disease (RDD) and JXG are non-LCHs but lack foamy macrophages.^{7,9} Moreover, RDD lesions exhibit emperipolesis and strong S-100 positivity, and JXG does not involve the long bones.⁷ Finally, both RDD and JXG can have a benign course or exhibit regression³¹⁻³³; for ECD, progression is nearly universal if untreated, and no case of regression has been documented.

Misdiagnosis can allow morbidities such as lower extremity bone pain, polyuria, polydipsia, fatigue, and chronic inflammation to progress. When ECD tumors grow unabated, retroperitoneal masses cause renal failure, orbital tumors threaten vision, pulmonary fibrosis can lead to pulmonary failure and cardiac complications, cerebellar lesions cause ataxia and dysarthria, and cardiac tumors result in pericardial effusions.

No approved therapies exist for ECD, and the results of empiric therapy have been disappointing. The most common treatments involve either standard doses of interferon α (3-9 million units; 135 μ g, pegylated form) weekly or high-dose interferon α (≥ 9 million units; >180 μ g, pegylated form).^{11,12} Other therapies include steroids,¹⁵ imatinib,¹⁶ anakinra,¹⁰ and cladribine^{17,18} and, less frequently, rapamycin¹⁴ and methotrexate.¹⁹ In our cohort, a partial response was seen in only 10% of treated cases; most remained stable, and 38% had been living with ECD for ≥ 3 years. The most common drug side effects were fever, anorexia, fatigue, and weakness and occasionally immunosuppression and/or bone marrow suppression. One patient treated with interferon α developed sarcoidosis. A multispecialty team is needed for the adequate management of a patient with ECD in order to address the numerous manifestations secondary to the disease. Neurological and cardiac manifestations need special attention due to their association with increased morbidity, mortality, and challenging management. Since ECD cardiovascular involvement is often asymptomatic, patients should be evaluated by cardiac MRI or CT or both.³⁴ Although MRI enables tissue characterization, the availability of cardiac MRI is

much more limited than CT, which provides superior resolution and anatomical detail. Additionally, due to significantly longer examination times and metallic contraindications for MRI, patients tolerate CT examinations more often. Endocrine abnormalities also need adequate assessment because of their varied presentation and severity. Evidence of osteosclerosis in the mandible was found in 47% of our cases. Though asymptomatic, a comprehensive dental evaluation is indicated in patients with ECD.

Recent therapies reflect the new understanding of the molecular bases of ECD histiocytosis. The disease arises from somatic mutations occurring at a relatively specific point in monocyte cell differentiation, with subsequent random distribution of cells to distant sites. The array of monocyte-specific markers, combined with the many tissues affected, supports this assertion. Children are rarely affected with ECD. In our cohort, the mean age at presentation was 46 years, and half of patients did not develop bone, lung, retroperitoneal, retro-orbital, cardiac, or pituitary involvement until ~60 years of age. Germline mutations are unlikely to cause ECD, since no 2 members of a family have ever been reported with ECD, and affected individuals do not have oncogene mutations in nonhistiocytic cells. In our cohort, no germline mutations were identified. Rather, approximately half of our patients had monoallelic *BRAF* V600E mutations in affected tissues. Consistent with reports of other MAPK pathway mutations, we also identified an *ARAF*²¹⁻²³ mutation. These findings indicate that despite the presence of inflammatory markers and the absence of metastases, ECD must be considered a neoplasm and has been designated as such by the World Health Organization classification, and it needs to be adopted by the field of oncology. In addition, *BRAF* and *MEK* inhibitors can provide new hope for treating ECD and improve survival. Efficacy has been reported with vemurafenib,^{24,25} and a Cancer Therapy Evaluation Program–sponsored therapeutic trial of dabrafenib and trametinib is enrolling new ECD patients with *BRAF* V600E mutations (www.clinicaltrials.gov #NCT02281760). The discovery of new genes associated with ECD and the advances made in the management of this disease prompt an update to the consensus guidelines written by Diamond et al in 2014.⁷ Finally, knowledge of the molecular defects in ECD allows the creation of animal models and immortal cell lines for targeting critical components of the pathway.

References

1. Chester W. Uber Lipoidgranulomatose. *Virchows Arch Pathol Anat.* 1930;279:561-602.
2. Emile JF, Ablu O, Fraitag S, et al; Histiocyte Society. Revised classification of histiocytoses and neoplasms of the macrophage-dendritic cell lineages. *Blood.* 2016;127(22):2672-2681.
3. Veysier-Belot C, Cacoub P, Caparros-Lefebvre D, et al. Erdheim-Chester disease. Clinical and radiologic characteristics of 59 cases. *Medicine (Baltimore).* 1996;75(3):157-169.
4. Haroche J, Arnaud L, Cohen-Aubart F, et al. Erdheim-Chester disease. *Curr Rheumatol Rep.* 2014;16(4):412.
5. Campochiaro C, Tomelleri A, Cavalli G, Berti A, Dagna L. Erdheim-Chester disease. *Eur J Intern Med.* 2015;26(4):223-229.
6. Swerdlow SH, Campo E, Pileri SA, et al. The 2016 revision of the World Health Organization classification of lymphoid neoplasms. *Blood.* 2016;127(20):2375-2390.
7. Diamond EL, Dagna L, Hyman DM, et al. Consensus guidelines for the diagnosis and clinical management of Erdheim-Chester disease. *Blood.* 2014;124(4):483-492.
8. Mazor RD, Manevich-Mazor M, Shoenfeld Y. Erdheim-Chester Disease: a comprehensive review of the literature. *Orphanet J Rare Dis.* 2013;8:137.

Acknowledgments

The authors appreciate the cooperation of the ECD patients and of the Erdheim-Chester Disease Global Alliance.

This work was supported in part by the Intramural Research programs of the National Institutes of Health National Human Genome Research Institute; the National Heart, Lung, and Blood Institute; the National Institute of Dental and Craniofacial Research; the Center for Cancer Research, National Cancer Institute; and the National Institutes of Health Clinical Center in Bethesda, MD.

The funding sources had no role in the study design, data collection, data analysis, or writing of the report.

Authorship

Contribution: J.I.E.-V. and W.A.G. conceptualized and designed the clinical research protocol; J.I.E.-V., K.J.O., and W.A.G. were the primary clinical staff involved in patient care, evaluation, and clinical data gathering; J.I.E.-V., L.C.B., K.J.O., and W.A.G. were involved in clinical data gathering and analysis; R.H.D., L.C.B., P.J.G., and B.R.G. were involved in clinical evaluations and data gathering; L.X. and M.R. were involved in experiment design and analysis for *BRAF* V600E detection through pyrosequencing; B.H.D. and O.A.-W. were involved in experiment design and analysis for *BRAF* wild-type ECD cases; A.A.M. and M.Y.C. were involved in clinical radiology, imaging collection, and interpretation; J.R.A.E. and N.S. were involved in chart review, clinical data gathering, and analysis; E.S.J. was involved in case pathology review and interpretation; J.I.E.-V. and W.A.G. wrote the manuscript; and J.I.E.-V. had full access to the study data and final responsibility for the decision to submit for publication.

Conflict-of-interest disclosure: The authors declare no competing financial interests.

ORCID profiles: J.I.E.-V., 0000-0002-2372-0372; L.C.B., 0000-0003-1021-0952; R.H.D., 0000-0003-1926-4105; B.H.D., 0000-0001-8090-5448; M.Y.C., 0000-0003-0743-9369; O.A.-W., 0000-0002-3907-6171; E.S.J., 0000-0003-4632-0301.

Correspondence: Juvianee I. Estrada-Veras, Section on Human Biochemical Genetics, Medical Genetics Branch, National Human Genome Research Institute, National Institutes of Health, 10 Center Dr, Building 10, Room 3-2551, Bethesda, MD 20892; e-mail: estradaverasji@mail.nih.gov.

9. Jaffe R. The histiocytoses. *Clin Lab Med*. 1999;19(1):135-155.
10. Aouba A, Georgin-Lavialle S, Pagnoux C, et al. Rationale and efficacy of interleukin-1 targeting in Erdheim-Chester disease. *Blood*. 2010;116(20):4070-4076.
11. Braiteh F, Boxrud C, Esmaili B, Kurzrock R. Successful treatment of Erdheim-Chester disease, a non-Langerhans-cell histiocytosis, with interferon-alpha. *Blood*. 2005;106(9):2992-2994.
12. Hervier B, Arnaud L, Charlotte F, et al. Treatment of Erdheim-Chester disease with long-term high-dose interferon- α . *Semin Arthritis Rheum*. 2012;41(6):907-913.
13. Munoz J, Janku F, Cohen PR, Kurzrock R. Erdheim-Chester disease: characteristics and management. *Mayo Clin Proc*. 2014;89(7):985-996.
14. Gianfreda D, Nicastro M, Galetti M, et al. Sirolimus plus prednisone for Erdheim-Chester disease: an open-label trial. *Blood*. 2015;126(10):1163-1171.
15. Bourke SC, Nicholson AG, Gibson GJ. Erdheim-Chester disease: pulmonary infiltration responding to cyclophosphamide and prednisolone. *Thorax*. 2003;58(11):1004-1005.
16. Janku F, Amin HM, Yang D, Garrido-Laguna I, Trent JC, Kurzrock R. Response of histiocytoses to imatinib mesylate: fire to ashes. *J Clin Oncol*. 2010;28(31):e633-e636.
17. Adam Z, Koukalová R, Sprláková A, et al. Successful treatment of Erdheim-Chester disease by 2-chlorodeoxyadenosine-based chemotherapy. Two case studies and a literature review [in Czech]. *Vnitř Lek*. 2011;57(6):576-589.
18. Adam Z, Sprláková A, Reháč Z, et al. Partial regression of CNS lesions of Erdheim-Chester disease after treatment with 2-chlorodeoxyadenosine and their full remission following treatment with lenalidomide [in Czech]. *Klin Onkol*. 2011;24(5):367-381.
19. Ho P, Smith C. High-dose methotrexate for the treatment of relapsed central nervous system Erdheim-Chester disease. *Case Rep Hematol*. 2014;2014:269359.
20. Jeon IS, Lee SS, Lee MK. Chemotherapy and interferon-alpha treatment of Erdheim-Chester disease. *Pediatr Blood Cancer*. 2010;55(4):745-747.
21. Haroche J, Charlotte F, Arnaud L, et al. High prevalence of BRAF V600E mutations in Erdheim-Chester disease but not in other non-Langerhans cell histiocytoses. *Blood*. 2012;120(13):2700-2703.
22. Diamond EL, Durham BH, Haroche J, et al. Diverse and targetable kinase alterations drive histiocytic neoplasms. *Cancer Discov*. 2016;6(2):154-165.
23. Emile JF, Diamond EL, Hélias-Rodzewicz Z, et al. Recurrent RAS and PIK3CA mutations in Erdheim-Chester disease. *Blood*. 2014;124(19):3016-3019.
24. Hyman DM, Puzanov I, Subbiah V, et al. Vemurafenib in multiple nonmelanoma cancers with BRAF V600 mutations. *N Engl J Med*. 2015;373(8):726-736.
25. Haroche J, Cohen-Aubart F, Emile JF, et al. Dramatic efficacy of vemurafenib in both multisystemic and refractory Erdheim-Chester disease and Langerhans cell histiocytosis harboring the BRAF V600E mutation. *Blood*. 2013;121(9):1495-1500.
26. Haroche J, Cohen-Aubart F, Emile JF, et al. Reproducible and sustained efficacy of targeted therapy with vemurafenib in patients with BRAF(V600E)-mutated Erdheim-Chester disease. *J Clin Oncol*. 2015;33(5):411-418.
27. Bianco F, Iacovelli E, Tinelli E, Locuratolo N, Pauri F, Fattapposta F. Characteristic brain MRI appearance of Erdheim-Chester disease. *Neurology*. 2009;73(24):2120-2122.
28. Bassou D, El Kharras A, Taoufik AT, et al. Cardiac Erdheim-Chester. *Intern Med*. 2009;48(1):83-84.
29. Drier A, Haroche J, Savatovsky J, et al. Cerebral, facial, and orbital involvement in Erdheim-Chester disease: CT and MR imaging findings. *Radiology*. 2010;255(2):586-594.
30. Lachenal F, Cotton F, Desmurs-Clavel H, et al. Neurological manifestations and neuroradiological presentation of Erdheim-Chester disease: report of 6 cases and systematic review of the literature. *J Neurol*. 2006;253(10):1267-1277.
31. Vuong V, Moulouguet I, Cordoliani F, et al. Cutaneous revelation of Rosai-Dorfman disease: 7 cases [in French]. *Ann Dermatol Venereol*. 2013;140(2):83-90.
32. Miyake Y, Ito S, Tanaka M, Tanaka Y. Spontaneous regression of infantile dural-based non-Langerhans cell histiocytosis after surgery: case report. *J Neurosurg Pediatr*. 2015;15(4):372-379.
33. Chang SE, Cho S, Choi JC, et al. Clinicohistopathologic comparison of adult type and juvenile type xanthogranulomas in Korea. *J Dermatol*. 2001;28(8):413-418.
34. Haroche J, Cluzel P, Toledano D, et al. Images in cardiovascular medicine. Cardiac involvement in Erdheim-Chester disease: magnetic resonance and computed tomographic scan imaging in a monocentric series of 37 patients. *Circulation*. 2009;119(25):e597-e598.